

Thermally Two-stepped Spin Transitions Induced by Intramolecular Electron Transfers in a Cyanide-bridged Molecular Square

Masayuki Nihei, Yoshihiro Sekine, Naoki Suganami, and Hiroki Oshio*

Graduate School of Pure and Applied Sciences, University of Tsukuba, 1-1-1 Tennodai, Tsukuba, Ibaraki 305-8571

(Received July 2, 2010; CL-100604; E-mail: oshio@chem.tsukuba.ac.jp)

A cyanide-bridged molecular square, $[\text{Co}_2\text{Fe}_2(\text{CN})_6(\text{tp}^*)_2(\text{dtbbpy})_4](\text{PF}_6)_2 \cdot 2\text{MeOH}$ (**1**) (tp^* = hydrotris(3,5-dimethylpyrazol-1-yl) borate and dtbbpy = 4,4'-di-*tert*-butyl-2,2'-bipyridine) was prepared by the reaction of $(\text{Bu}_4\text{N})[\text{Fe}(\text{CN})_3(\text{tp}^*)]$ with $\text{Co}(\text{CF}_3\text{SO}_3)_2 \cdot 6\text{H}_2\text{O}$ and dtbbpy in methanol. Variable temperature X-ray structural analyses, magnetic and spectroscopic data revealed that **1** exhibited novel thermal two-stepped spin transitions induced by intramolecular electron transfers.

Prussian blue analogs (PBAs) are 3-D bulk materials with face-centered cubic structures, where metal ions with various electronic and oxidation states are bridged by cyanide ions. Cyanide ions mediate electronic and magnetic interactions between metal ions, some of which allow PBA to exhibit fruitful physical properties, such as high T_c magnets, spin-crossover, linkage isomerism, and ferroelectric properties.¹ In 1996, Hashimoto and co-workers observed a photoinduced magnetization in $\text{K}_{0.2}\text{Co}_{1.4}[\text{Fe}(\text{CN})_6] \cdot 6.9\text{H}_2\text{O}$,² in which light irradiation induces electron transfers from Fe(II) to Co(III) ions stimulating spin transition from low-spin (LS) to high-spin (HS) states on the Co ions, called charge-transfer-induced spin transition (CTIST).³ On the other hand, cyanide-bridged multinuclear complexes have core structures similar to a constituent unit of PBA, and such complexes have potential to show specific molecular functions, such as single-molecular magnetism, multi-stepped spin-crossover, and multisteped redox behavior.⁴ Dunbar and co-workers have reported the first observation of gradual CTIST behavior in a discrete molecule, that is, a cyanide-bridged pentanuclear Fe–Co cluster with a trigonal-bipyramidal core.⁵ Although there are few reports on other complexes exhibiting one-step CTISTs,⁶ to the best of our knowledge, there have been no reports of the two-stepped CTIST behavior in both bulk and discrete molecular systems. We report here a novel cyanide-bridged molecular square of $[\text{Co}_2\text{Fe}_2(\text{CN})_6(\text{tp}^*)_2(\text{dtbbpy})_4](\text{PF}_6)_2 \cdot 2\text{MeOH}$ (**1**) (tp^* = hydrotris(3,5-dimethylpyrazol-1-yl) borate, dtbbpy = 4,4'-di-*tert*-butyl-2,2'-bipyridine), exhibiting a two-stepped CTIST.

1 was prepared by the reaction of $(\text{Bu}_4\text{N})[\text{Fe}^{\text{III}}(\text{CN})_3(\text{tp}^*)]$ with $\text{Co}^{\text{II}}(\text{CF}_3\text{SO}_3)_2 \cdot 6\text{H}_2\text{O}$ and dtbbpy in methanol.⁷ X-ray crystal structure analysis for **1** was performed at 100 K and an ORTEP diagram of the complex cation is depicted in Figure 1.⁸ **1** has a square-shaped macrocyclic core, in which Fe and Co ions are alternately bridged by cyanide ions. **1** crystallized in a monoclinic space group $C2/c$ and the asymmetric unit is composed of half of the complex cation, $[(\text{tp}^*)\text{Fe}(\text{CN})_3\text{Co}(\text{dtbbpy})_2]$. The Fe ions are coordinated by tridentate tp^* with facial configuration and the remaining coordination sites are occupied by three cyanide carbon atoms.

The two bidentate dtbbpy ligands coordinate to the Co ion, and bridging cyanide ions in *cis*-positions are linked to the

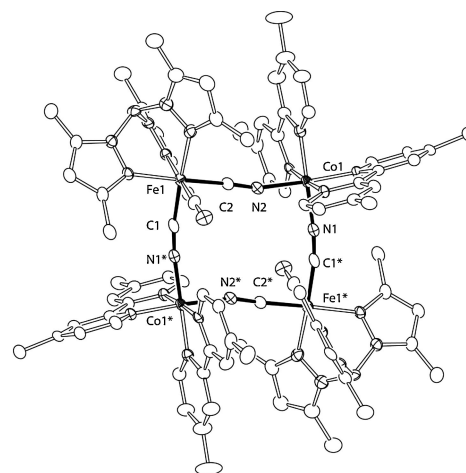


Figure 1. ORTEP diagram of a cation in **1**. Peripheral methyl groups on dtbbpy ligands were omitted for clarity.

neighboring $[(\text{tp}^*)\text{Fe}]$ units. The coordination bond lengths about the Co ion at 100 K are in the range of 1.892(7)–1.944(6) Å, characteristic of LS Co(III) ions. The average coordination bond length around the Fe centers is 1.959(7) Å, which corresponds to a LS Fe(II) or LS Fe(III) ion. Although the assignments of oxidation states of LS Fe(II) and Fe(III) ions are difficult only from the structural data, Mössbauer measurements (Figure S1)⁹ confirmed that the Fe centers in **1** can be assigned as LS Fe(II) ions (*vide infra*), and the electronic structure can be described as $[\text{Fe}^{\text{II}}_{\text{LS}_2}\text{Co}^{\text{III}}_{\text{LS}_2}]$ at 20 K.

Magnetic susceptibility measurements were performed on **1** in the temperature range of 5–330 K (Figure 2). The $\chi_m T$ values below 250 K are nearly constant with a value of 0.18 $\text{emu mol}^{-1}\text{K}$ at 250 K, suggesting that **1** is almost in the diamagnetic electronic state of $[\text{Fe}^{\text{II}}_{\text{LS}_2}\text{Co}^{\text{III}}_{\text{LS}_2}]$; the LT phase. As the temperature is increased from 250 to 330 K, the $\chi_m T$ values increased in a two-step fashion centered at 275 and 310 K, indicating the occurrence of CTIST from the LT to a high-temperature (HT) phase via an intermediate (IM) phase. The $\chi_m T$ value at 330 K (HT phase) is 6.55 $\text{emu mol}^{-1}\text{K}$, which is in agreement with the Curie constant (6.32 $\text{emu mol}^{-1}\text{K}$) expected for the value of $[\text{Fe}^{\text{III}}_{\text{LS}_2}\text{Co}^{\text{II}}_{\text{HS}_2}]$, that is, two noncorrelated LS Fe(III) ($S = 1/2$ with $g = 2.7$) and two HS Co(II) ($S = 3/2$ with $g = 2.3$) ions.⁶ The IM phase has a $\chi_m T$ value of 3.33 $\text{emu mol}^{-1}\text{K}$ at 296 K, which is almost half of the value in the HT phase. Note that $\chi_m T$ values in the cooling mode traced the profile in the heating mode and no magnetic hysteresis was observed.

⁵⁷Fe Mössbauer spectra of **1** were measured at 20, 280, and 320 K to characterize the electronic states of the iron ions in each phase (Figure S1).⁹ A quadrupole doublet was observed at 20 K

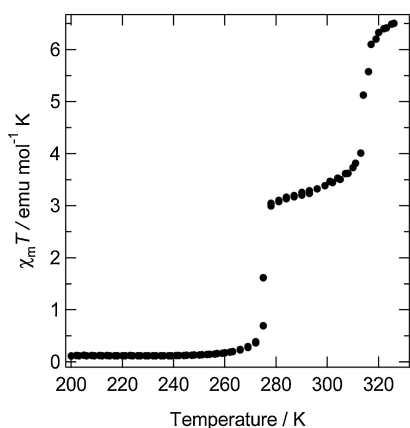


Figure 2. $\chi_m T$ - T plot for **1**.

(LT phase), and its Mössbauer parameters ($\delta = 0.22$ and $\Delta E_Q = 0.43 \text{ mm s}^{-1}$),¹⁰ characteristic of diamagnetic LS Fe(II) species, suggested that **1** is in the diamagnetic LT phase. As the temperature was raised to 280 K, an additional doublet with $\delta = 0.04$ and $\Delta E_Q = 0.90 \text{ mm s}^{-1}$, corresponding to LS iron(III) species, was observed. The peak area ratio of Fe(II) to Fe(III) species is 0.50/0.50 at 280 K, suggesting that half of the iron(II) ions are oxidized to iron(III) due to CTIST in the IM phase. In the HT phase at 320 K, a LS Fe(III) doublet with $\delta = 0.00$ and $\Delta E_Q = 0.91 \text{ mm s}^{-1}$ was dominant, suggesting complete CTIST from the $[\text{Fe}^{\text{II}}_{\text{LS}_2}\text{Co}^{\text{III}}_{\text{LS}_2}]$ to the $[\text{Fe}^{\text{III}}_{\text{LS}_2}\text{Co}^{\text{II}}_{\text{HS}_2}]$ occurred in the HT phase.

Further X-ray crystal structural analyses were carried out at 298 K (IM phase) and 330 K (HT phase). Although the space groups at both temperatures remained $C2/c$, the coordination bond lengths were significantly different. In the HT phase at 330 K, the average coordination bond lengths about the Co and Fe ions are 2.113(4) and 1.964(5) Å, respectively, suggesting the complete CTIST from the LT phase to the HT phase. The average coordination bond length about Co ions is 2.020(5) Å at 298 K which lie in the middle range of the typical bond lengths for LS Co(III) (1.925(6) Å) and HS Co(II) ions (2.113(4) Å). The observed bond lengths at 298 K might be due to the positional disorder of LS Co(III) and HS Co(II) ions on the asymmetric site or missing the weak superlattice reflections originating from long-range order.

All data described above suggested that the possible electronic structures of **1** in the IM phase are either $[\text{Fe}^{\text{III}}_{\text{LS}}\text{Fe}^{\text{II}}_{\text{LS}_2}\text{Co}^{\text{III}}_{\text{LS}}\text{Co}^{\text{II}}_{\text{HS}}]$ or a 1:1 mixture of $[\text{Fe}^{\text{II}}_{\text{LS}_2}\text{Co}^{\text{III}}_{\text{LS}_2}]$ and $[\text{Fe}^{\text{III}}_{\text{LS}_2}\text{Co}^{\text{II}}_{\text{HS}_2}]$. To prove the electronic structure of **1** in the IM phase, variable temperature infrared (IR) absorption spectra were measured (Figure S2).⁹ IR spectroscopy is a useful tool to characterize the electronic states of cyanide-bridged metal ions, because stretching frequencies of cyanide groups (ν_{CN}) are sensitive to the oxidation states of bridged metals ions. In the HT phase **1** exhibited a ν_{CN} absorption peak at 2152 cm^{-1} , which is a typical value of $\text{Fe}^{\text{III}}_{\text{LS}}-(\mu\text{-CN})-\text{Co}^{\text{II}}_{\text{HS}}$ bridges.⁵ The ν_{CN} absorption peak was therefore assigned to the stretching of the bridging cyanide ions in the $[\text{Fe}^{\text{III}}_{\text{LS}_2}\text{Co}^{\text{II}}_{\text{HS}_2}]$ electronic state, which is in accord with the Mössbauer data. With decreasing temperature, new ν_{CN} peaks were observed at 2096 and 2077 cm^{-1} , which are characteristic of $\text{Fe}^{\text{II}}-(\mu\text{-CN})-\text{Co}^{\text{III}}$ linkages in the LT phase ($[\text{Fe}^{\text{II}}_{\text{LS}_2}\text{Co}^{\text{III}}_{\text{LS}_2}]$).⁵ No additional peaks

were observed, which rules out the electronic structure of $[\text{Fe}^{\text{III}}_{\text{LS}}\text{Fe}^{\text{II}}_{\text{LS}_2}\text{Co}^{\text{III}}_{\text{LS}}\text{Co}^{\text{II}}_{\text{HS}}]$, and the IM phase is, therefore, considered to be 1:1 mixture of $[\text{Fe}^{\text{II}}_{\text{LS}_2}\text{Co}^{\text{III}}_{\text{LS}_2}]$ and $[\text{Fe}^{\text{III}}_{\text{LS}_2}\text{Co}^{\text{II}}_{\text{HS}_2}]$ species.

In summary, the cyanide-bridged molecular square **1** was prepared and the first two-stepped CTIST behavior was observed. Although the nature of the IM phase is still unclear, spectroscopic data suggested that the IM phase contains HS and LS molecules in 1:1 ratio. X-ray diffraction measurements using synchrotron radiation are currently underway to determine the detailed structure the IM phase.

This work was supported by a Grant-in-Aid for Scientific Research on Innovative Areas ("Coordination Programming" Area 2107, No. 21108006) from MEXT, Japan.

References and Notes

- 1 a) T. Mallah, S. Thiébaud, M. Verdaguer, P. Veillet, *Science* **1993**, *262*, 1554. b) S. Ferlay, T. Mallah, R. Ouahès, P. Veillet, M. Verdaguer, *Nature* **1995**, *378*, 701. c) W. E. Buschmann, J. Enslin, P. Gülich, J. S. Miller, *Chem.—Eur. J.* **1999**, *5*, 3019. d) E. Coronado, M. C. Giménez-López, G. Levchenko, F. M. Romero, V. García-Baonza, A. Milner, M. Paz-Pasternak, *J. Am. Chem. Soc.* **2005**, *127*, 4580. e) W. Kosaka, K. Nomura, K. Hashimoto, S. Ohkoshi, *J. Am. Chem. Soc.* **2005**, *127*, 8590. f) S. Ohkoshi, H. Tokoro, T. Matsuda, H. Takahashi, H. Irie, K. Hashimoto, *Angew. Chem., Int. Ed.* **2007**, *46*, 3238.
- 2 O. Sato, T. Iyoda, A. Fujishima, K. Hashimoto, *Science* **1996**, *272*, 704.
- 3 N. Shimamoto, S. Ohkoshi, O. Sato, K. Hashimoto, *Inorg. Chem.* **2002**, *41*, 678.
- 4 a) E. J. Schelter, F. Karadas, C. Avendano, A. V. Prosvirin, W. Wernsdorfer, K. R. Dunbar, *J. Am. Chem. Soc.* **2007**, *129*, 8139. b) M. Nihei, M. Ui, M. Yokota, L. Han, A. Maeda, H. Kishida, H. Okamoto, H. Oshio, *Angew. Chem., Int. Ed.* **2005**, *44*, 6484. c) J. J. Sokol, A. G. Hee, J. R. Long, *J. Am. Chem. Soc.* **2002**, *124*, 7656. d) M. Nihei, M. Ui, N. Hoshino, H. Oshio, *Inorg. Chem.* **2008**, *47*, 6106.
- 5 C. P. Berlinguette, A. Dragulescu-Andrasi, A. Sieber, J. R. Galán-Mascarós, H.-U. Güdel, C. Achim, K. R. Dunbar, *J. Am. Chem. Soc.* **2004**, *126*, 6222.
- 6 a) D. Li, R. Clérac, O. Roubeau, E. Harté, C. Mathonière, R. L. Bris, S. M. Holmes, *J. Am. Chem. Soc.* **2008**, *130*, 252. b) M. G. Hilfiger, M. Chen, T. V. Brinzari, T. M. Nocera, M. Shatruk, D. T. Petais, J. L. Musfeldt, C. Achim, K. R. Dunbar, *Angew. Chem., Int. Ed.* **2010**, *49*, 1410. c) Y. Zhang, D. Li, R. Clérac, M. Kalisz, C. Mathonière, S. M. Holmes, *Angew. Chem., Int. Ed.* **2010**, *49*, 3752.
- 7 Yield: 30%. Anal. Calcd for $\text{C}_{110}\text{H}_{148}\text{B}_2\text{Co}_2\text{F}_{12}\text{Fe}_2\text{N}_{26}\text{O}_2\text{P}_2$: C, 54.88; H, 6.20; N, 15.13%. Found: C, 54.73; H, 6.12; N, 15.22.
- 8 Crystal data for **1** at 100 K: $\text{C}_{110}\text{H}_{148}\text{B}_2\text{Co}_2\text{F}_{12}\text{Fe}_2\text{N}_{26}\text{O}_2\text{P}_2$, monoclinic $C2/c$, $a = 24.556(4) \text{ \AA}$, $b = 18.762(3) \text{ \AA}$, $c = 29.255(5) \text{ \AA}$, $\beta = 113.427(2)^\circ$, $V = 12367(4) \text{ \AA}^3$, $Z = 8$, $d_{\text{calcd}} = 1.293 \text{ Mg m}^{-3}$, 26997 reflections measured, 8904 unique reflections ($R_{\text{int}} = 0.0958$). Final $R1 = 0.0647$ and $wR2 = 0.1673$ ($I > 2\sigma I$); at 298 K: monoclinic $C2/c$, $a = 24.724(3) \text{ \AA}$, $b = 19.233(2) \text{ \AA}$, $c = 29.883(3) \text{ \AA}$, $\beta = 113.790(2)^\circ$, $V = 13003(2) \text{ \AA}^3$, $Z = 8$, $d_{\text{calcd}} = 1.230 \text{ Mg m}^{-3}$, 29496 reflections measured, 9624 unique reflections ($R_{\text{int}} = 0.0441$). Final $R1 = 0.0642$ and $wR2 = 0.1831$ ($I > 2\sigma I$); at 330 K: monoclinic $C2/c$, $a = 24.5679(16) \text{ \AA}$, $b = 19.6771(13) \text{ \AA}$, $c = 30.1520(19) \text{ \AA}$, $\beta = 114.0180(10)^\circ$, $V = 13314.2(19) \text{ \AA}^3$, $Z = 8$, $d_{\text{calcd}} = 1.201 \text{ Mg m}^{-3}$, 33027 reflections measured, 11076 unique reflections ($R_{\text{int}} = 0.0366$). Final $R1 = 0.0734$ and $wR2 = 0.2085$ ($I > 2\sigma I$).
- 9 Supporting Information is available electronically on the CSJ-Journal Web site, <http://www.csj.jp/journals/chem-lett/index.html>.
- 10 Mössbauer parameters were calculated relative to metallic iron.